

EXACT LOCALIZATION OF PLANAR ACOUSTIC REFLECTORS IN THREE-DIMENSIONAL GEOMETRIES

A. Canclini^b, F. Antonacci^b, J. Filos[‡], A. Sarti^b, P. Naylor[‡]

^b Politecnico di Milano, p.zza Leonardo da Vinci 32, 20133 Milano, Italy

[‡] Imperial College London, Exhibition Road, London SW7 2AZ, UK

ABSTRACT

In this paper we propose a methodology for localizing acoustic planar reflectors in a 3D geometry, using acoustic measurements acquired by a set of microphones. An acoustic source emitting a known signal is placed close to the wall to be identified, and is used for estimating the source-to-microphone impulse responses. In a preliminary step, such estimates are employed for localizing the source. After that, the Times Of Arrival (TOAs) associated to the first order reflective paths are extracted from the impulse responses and converted into quadratic constraints (ellipsoids) acting on the reflective plane. The constraints are then collected into a cost function, whose exact minimization leads to the searched plane. A theoretical analysis is performed for predicting the impact of measurement errors on the estimation. Moreover, experimental results in a real meeting room prove the effectiveness of the method.

Index Terms— Microphone arrays, acoustic reflector localization, room geometry estimation

1. INTRODUCTION

In this paper we discuss the problem of the localization of reflectors in a 3D geometry through the use of acoustic measurements. More specifically, we propose here a technique for the localization of reflectors using an exact minimization of the cost function that underlies the localization of the reflector. The problem of estimating the 3D geometry of environments has been already studied in [1], [2] and [3]. In [3] the authors localize the reflectors through the localization of the real and image sources by a compact microphone array. This methodology is interesting because it is not invasive, as only a loudspeaker and a small array are used. However, when the accuracy of the reconstruction is important, this technique could prove unsuitable. This is because the small size of the microphone array hinders a sufficient resolution in the localization of the sources, thus making the overall estimate of the shape of the room inaccurate. In [1] the authors approach the localization of planar reflectors by extending the approach originally adopted in [4] to 3D geometries. However, the cost function employed presents several local minima, in which the minimization could get trapped into. In order to prevent this problem, a generalized Hough transform is used, which provides an initial estimate. In [2] a different route is followed. Here the localization of 3D reflectors is achieved by combining multiple 2D estimates. In particular, a cross-array is decomposed into sub-arrays, each of which lies on one of the three planes xz , yz and xy . The localization of the portion of the reflector lying on each of the three planes (i.e. a line) is performed through the analysis of the signals coming from each sub-array. In a later stage linear estimates are combined through a least-squares technique to find the actual pa-

rameters of the 3D reflector. A Hough transform (defined differently from [1]) is adopted in order to prevent the problem of local minima.

In this paper we intend to remove the need of an initial estimate for the reflector estimate, thus reducing the computational cost and making the algorithm more robust against measurement errors. At this purpose, in [5] the authors have implemented a technique for the localization of reflectors in 2D which employs an exact minimization of the cost-function. The key point is that the cost function, a fourth-order polynomial, can be reformulated as a second-order polynomial with a single quadratic constraint, which admits an exact solution. This approach guarantees that the true reflector is found and local minima are avoided. In this paper we extend the approach proposed in [5] to 3D geometries. Even if this extension is quite smooth, it represents a relevant novelty, as it removes the need of an initial estimate. The analysis on the data acquired in a small conference room confirms that the proposed technique is able to localize the reflectors with a distance error of a few centimeters and an angular error below one degree. In [5] the authors also presented a methodology for the analytical prediction of the impact of errors on measurements on the localization error. This research theme is becoming increasingly important, as demonstrated by recent publications (e.g. [6] and [7]) where the authors study the problem of the propagation of error measurements into the estimation process, taking inspiration from the Information Geometry [8].

The novel contributions of this work with respect to the literature are: the extension of the closed-form solution to 3D geometries; and the extension to the 3D case of the prediction of the impact of measurement errors on the localization accuracy.

The rest of the paper is structured as follows: section 2 formulates the problem of localization of reflectors in 3D; section 3 briefly explains how the acoustic source is localized prior to localizing reflectors, adopting the same approach introduced in [9]. Section 4 proposes the solution adopted for the localization of reflectors. The theoretical analysis of error propagation and some experimental results based on real data are proposed in section 5. Finally, section 6 draws some conclusions.

2. PROBLEM FORMULATION

We consider an acoustic scene in which a set of M microphones, located at $\mathbf{x}_m = [x_m, y_m, z_m]^T$, $m = 1, \dots, M$, possibly organized in an array, capture, after A/D conversion, the time-discrete sound $x_{ms}(n)$, $m = 1, \dots, M$ produced by a source $s(n)$, which occupies the positions $\mathbf{x}_s = [x_s, y_s, z_s]^T$, $s = 1, \dots, S$. We assume that the number of source positions S is equal to the number of planar reflective surfaces to be localized. In the illustrative example in Fig. 1, a single reflector and source are present in the acoustic scene. Reflectors are represented by the coordinates of the plane on which they

lie. In particular, points on the plane $\mathbf{P} = [p_1, p_2, p_3, p_4]^T$ satisfy the equation

$$p_1x + p_2y + p_3z + p_4 = \mathbf{P}^T \mathbf{x} = 0,$$

where $\mathbf{x} = [x, y, z, 1]^T$ are the homogeneous coordinates of the generic point $\mathbf{x} = [x, y, z]^T$ lying on the plane.

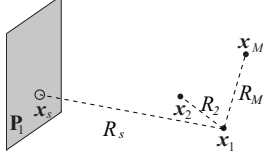


Fig. 1. Geometry of the problem of reflector localization

The signal $x_{ms}(n)$ can be modeled as the convolution of $s(n)$ with the discrete acoustic impulse response (AIR) of the room from \mathbf{x}_s to \mathbf{x}_m , denoted by $h_{ms}(n)$,

$$x_{ms}(n) = s(n) * h_{ms}(n). \quad (1)$$

We assume that the line of sight between microphones and sources is not occluded by obstacles. Therefore, the direct path between $\mathbf{x}_s, s = 1, \dots, S$ and $\mathbf{x}_m, m = 1, \dots, M$ is present in the impulse responses. Along with the direct path, reflective paths are also visible in the AIR. Let us now consider a specific source location \mathbf{x}_s . For this location we assume that in $h_{ms}(n)$ the first echo after the direct-path is related to the same reflector for $m = 1, \dots, M$. This assumption is satisfied if i) \mathbf{x}_s is sufficiently close to the reflector of interest and ii) microphones are compactly organized in space. If both conditions apply, we can write that

$$h_{ms}(n) = \alpha_{ms}^{(0)} \delta(n - n_{ms}^{(0)}) + \alpha_{ms}^{(1)} \delta(n - n_{ms}^{(1)}) + \sum_{k=2}^K \alpha_{ms}^{(k)} \delta(n - n_{ms}^{(k)}),$$

where $\alpha_{ms}^{(k)}$ is the attenuation along the direct ($k = 0$) or reflective ($k \geq 1$) path; $n_{ms}^{(k)}$ is the propagation delay; and K is the number of relevant reflections. Moreover, $n_{ms}^{(0)} < n_{ms}^{(1)} < \dots < n_{ms}^{(k)}$ for $k \geq 2$. The direct and the shortest reflective paths have been kept out the summation, as they constitute the input of the algorithm proposed in this paper.

The estimation $\hat{h}_{ms}(n)$ of the AIR is obtained using a supervised approach, by means of a MLS sequence. In order to enable the use of uncontrolled sources, we do not assume that the source is synchronized with the microphones. We can write, therefore, that

$$\hat{h}_{ms}(n) = h_{ms}(n - D_s) + \nu_{ms}(n),$$

where D_s is an unknown delay, and $\nu_{ms}(n)$ are independent identically distributed realizations of a zero-averaged Gaussian noise, modeling the estimation error.

The problem of localizing reflectors in 3D corresponds to finding the parameters \mathbf{P} of the planes on which the reflectors lie, given the noisy and delayed AIRs $\hat{h}_{ms}(n)$.

We notice that in $\hat{h}_{ms}(n)$ the Time Of Arrival (TOA) of echoes (direct and reflective ones) are not preserved due to the presence of the unknown delay D_s . However, the Time Difference of Arrival (TDOA) of echoes at all microphone pairs are preserved, as D_s is equal for all microphones. We start from this observation to localize the source using the TDOAs related to the direct path (see section

3). Once the source has been localized, we convert the TDOAs of the reflective paths into TOAs, as already presented in [9]. TOAs are then used to estimate the location of the reflectors in the room (section 4).

When multiple reflectors are present in the acoustic scene, multiple independent estimations are performed, by sequentially placing the source in the proximity of each wall to be localized, so that the first-order reflection from the desired wall immediately follows the direct-path echo.

3. SOURCE LOCALIZATION

In this section we show how the sound source can be localized using TDOA information captured by the microphones. In particular, we adopt the least-squares passive localization algorithm proposed in [10]. This algorithm was already adapted to the 2D case in [9].

Assume that the reference microphone ($m = 1$) is placed at the origin of the coordinate system, i.e., $\mathbf{x}_1 = [0 \ 0 \ 0]^T$. The distances from the origin to the m th microphone and the source are denoted by R_m and R_s , respectively, where

$$R_m \triangleq \|\mathbf{x}_m\| = \sqrt{x_m^2 + y_m^2 + z_m^2}, \quad m = 2, \dots, M$$

$$R_s \triangleq \|\mathbf{x}_s\| = \sqrt{x_s^2 + y_s^2 + z_s^2}.$$

The difference in the distances of microphones m and n from the source is the *range difference*, $d_{m,n}$, and is proportional to the TDOA of the direct-path between the m th and n th microphone, denoted τ_{mn} . If the speed of sound is c , then

$$d_{mn} = c \tau_{mn}. \quad (2)$$

The acoustic source location, as well as its range, can be estimated using least-squares. We observe that the correct source location should be at the intersection of a group of spheres. The centre of each sphere is equal to the location of the microphone and the radius of each sphere is related to the source-microphone distance. Therefore, the best estimate of the source location will be the point that yields the shortest distance to those spheres defined by the range differences and the hypothesized source range. From [10] we establish the distance D_m from the m th microphone to the source

$$\hat{D}_m = R_s + \hat{d}_{m1}, \quad (3)$$

where $(\hat{\cdot})$ denotes an observation based on the measured range difference. The error function is then defined as the difference between the measured and true values, which when putting the $M - 1$ errors together and writing them in a vector form gives

$$\mathbf{e}(\mathbf{r}_s) = \mathbf{K}\theta - \mathbf{1} \quad (4)$$

where $\mathbf{K} \triangleq [\mathbf{S} \mid \hat{\mathbf{d}}]$ and $\mathbf{S} \mid \hat{\mathbf{d}}$ indicates that \mathbf{S} and $\hat{\mathbf{d}}$ are stacked side-by-side with $\hat{\mathbf{d}} = [\hat{d}_{21}, \hat{d}_{31}, \dots, \hat{d}_{M1}]^T$ and

$$\mathbf{S} \triangleq \begin{bmatrix} x_2 & y_2 & z_2 \\ x_3 & y_3 & z_3 \\ \vdots & \vdots & \vdots \\ x_M & y_M & z_M \end{bmatrix}, \theta \triangleq \begin{bmatrix} x_s \\ y_s \\ z_s \\ R_s \end{bmatrix}, \mathbf{1} \triangleq \frac{1}{2} \begin{bmatrix} R_2^2 - \hat{d}_{21}^2 \\ R_3^2 - \hat{d}_{31}^2 \\ \vdots \\ R_M^2 - \hat{d}_{M1}^2 \end{bmatrix}.$$

The solution for θ is given by $\hat{\theta} = \mathbf{K}^\ddagger \mathbf{1}$, where $(\cdot)^\ddagger$ defines the pseudo-inverse [10].

4. REFLECTOR LOCALIZATION

In this Section we describe the methodology for localizing the reflector associated to the source located at \mathbf{x}_s , whose coordinates come from the source localization technique outlined in Section 3. Without loss of generality, we now translate the reference frame at the source, so that its position becomes $\mathbf{x}_s = [0, 0, 0]^T$. This simple transformation will turn out useful in determining an exact solution to the reflector localization problem. We notice, however, that the resulting estimate $\hat{\mathbf{P}}$ of the reflective plane refers to the source position, which changes for the different walls to be localized. Afterwards, therefore, we convert the estimated plane vectors to the original coordinate system.

Let $\tau_m = n_{ms}/F_s$ be the TOA associated to the first-order reflective path between the m th microphone and the source, and F_s the sample frequency. As noticed in [1], the reflection point $\mathbf{x}_m^{(P)}$ on the reflector is located on an ellipsoid having foci at \mathbf{x}_m and \mathbf{x}_s , and major axis equal to $r_m = c \tau_m$. Since $\mathbf{x}_s = [0, 0, 0]^T$, a generic point $\mathbf{x} = [x, y, z]^T$ on the ellipsoid satisfies $\|\mathbf{x} - \mathbf{x}_m\| + \|\mathbf{x}\| = r_m$. After some manipulations, as in [1, 5], the ellipsoid can be rewritten in the form $\mathbf{x}^T \mathbf{Q}_m \mathbf{x} = 0$, which represents a quadric surface in 3D. In particular, $\mathbf{x} = [x, 1]^T$ is the homogeneous representation of \mathbf{x} ; and \mathbf{Q}_m is a symmetric matrix containing the quadric parameters (see [1] for additional details). Since the plane of reflection is bound to be tangential to the ellipsoid \mathbf{Q}_m at $\mathbf{x}_m^{(P)}$ [1], it is convenient to adopt the dual representation of the quadric, namely $\mathbf{P}^T \mathbf{Q}_m^* \mathbf{P} = 0$, which is satisfied by all the planes $\mathbf{P} = [p_1, p_2, p_3, p_4]^T$ of equation $p_1 x + p_2 y + p_3 z + p_4 = 0$ tangential to the ellipsoid. Computing $\mathbf{Q}_m^* = \det(\mathbf{Q}_m) \mathbf{Q}_m^{-1}$ we obtain

$$\mathbf{Q}_m^* = \begin{bmatrix} a_m^* & 0 & 0 & \frac{d_m^*}{2} \\ 0 & a_m^* & 0 & \frac{g_m^*}{2} \\ 0 & 0 & a_m^* & \frac{i_m^*}{2} \\ \frac{d_m^*}{2} & \frac{g_m^*}{2} & \frac{i_m^*}{2} & l_m^* \end{bmatrix}, \quad \begin{aligned} a_m^* &= 16r_m^4(\|\mathbf{x}_m\|^2 - r_m^2)^2, \\ d_m^* &= 64r_m^4 x_m(\|\mathbf{x}_m\|^2 - r_m^2), \\ g_m^* &= 64r_m^4 y_m(\|\mathbf{x}_m\|^2 - r_m^2), \\ i_m^* &= 64r_m^4 z_m(\|\mathbf{x}_m\|^2 - r_m^2), \\ l_m^* &= 64r_m^4(\|\mathbf{x}_m\|^2 - r_m^2). \end{aligned}$$

The combination of M TOA measurements leads to the definition of the minimization problem

$$\hat{\mathbf{P}} = \underset{\mathbf{P}}{\operatorname{argmin}} J(\mathbf{P}) = \underset{\mathbf{P}}{\operatorname{argmin}} \sum_{m=1}^M \left(\mathbf{P}^T \mathbf{Q}_m^* \mathbf{P} \right)^2, \quad (5)$$

where the plane of reflection is estimated as the global minimum of the cost function $J(\mathbf{P})$, which is the sum of the squared residuals of all the quadratic constraints. Following the same approach proposed in [5] for reflector line estimation, we restrict the search space to planes having $p_4 = 1$. This means discarding all the planes passing through the origin, which can not generate any reflective path since they contain the source. As a result, we obtain

$$\hat{\mathbf{P}} = \underset{\mathbf{P}}{\operatorname{argmin}} \sum_{m=1}^M \left[a_m^* (p_1^2 + p_2^2 + p_3^2) + d_m^* p_1 + g_m^* p_2 + i_m^* p_3 + l_m^* \right]^2. \quad (6)$$

By posing $w = p_1^2 + p_2^2 + p_3^2$, (6) can be rewritten as the following *generalized trust region subproblem* (GTRS) [11]

$$\hat{\mathbf{w}} = \underset{\mathbf{w}}{\operatorname{argmin}} \left\{ \|\mathbf{A}\mathbf{w} - \mathbf{b}\|^2 : \mathbf{w}^T \mathbf{D}\mathbf{w} + 2\mathbf{f}^T \mathbf{w} = 0 \right\}, \quad (7)$$

where $\mathbf{w} = [w, p_1, p_2, p_3]^T$ and

$$\mathbf{A} = \begin{bmatrix} a_1^* & d_1^* & g_1^* & i_1^* \\ \vdots & \vdots & \vdots & \vdots \\ a_M^* & d_M^* & g_M^* & i_M^* \end{bmatrix}, \quad \begin{aligned} \mathbf{b} &= [-l_1^* \dots l_M^*]^T, \\ \mathbf{D} &= \operatorname{diag}(0, 1, 1, 1), \\ \mathbf{f} &= [-0.5 \ 0 \ 0 \ 0]^T. \end{aligned}$$

The exact solution $\hat{\mathbf{w}} = [\hat{w} \ \hat{p}_1 \ \hat{p}_2 \ \hat{p}_3]^T$ to (7) can be found efficiently as in [11, 5], and the searched plane of reflection is given by $\hat{\mathbf{P}} = [\hat{p}_1 \ \hat{p}_2 \ \hat{p}_3 \ 1]^T$, which is expressed in the source reference system. The solution in the original reference system is finally obtained as $\hat{\hat{\mathbf{P}}} = (\mathbf{T}_s^{-1})^T \hat{\mathbf{P}}$, where

$$\mathbf{T}_s = \begin{bmatrix} 1 & 0 & 0 & x_s \\ 0 & 1 & 0 & y_s \\ 0 & 0 & 1 & z_s \\ 0 & 0 & 0 & 1 \end{bmatrix}$$

denotes the translation from the original reference frame to that centered at $\mathbf{x}_s = [x_s, y_s, z_s]^T$.

5. RESULTS

In this Section we test the accuracy of the proposed 3D reflector localization technique. In particular, first we analyze the effect of the error on TOA measurements on the estimation. This is accomplished by means of the theoretical error propagation analysis proposed in [12] and adopted in [5] for the case of 2D reflector localization. After that, the algorithm is tested in a real meeting room, by comparing the estimated wall positions with the hand-measured ground truth.

5.1. Theoretical analysis

The theoretical analysis has been performed using the setup shown in Figure 2. For the sake of clarity in the analysis of the results, in this section we parametrize the reflective plane by its distance d from the origin (coincident with the source position \mathbf{x}_s); the azimuth ϕ ; and the co-elevation θ . The plane parametrization adopted

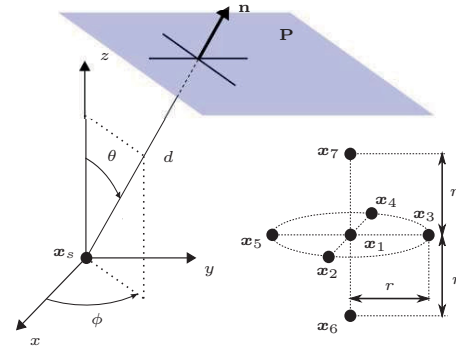


Fig. 2. Evaluation setup

in section 2 is related with the current one through $\mathbf{P} = [\mathbf{n}^T, d]^T$, $\mathbf{n} = [\cos \phi \sin \theta, \sin \phi \sin \theta, \cos \theta]^T$ being the unit vector normal to the plane. The microphone array accommodates 7 sensors deployed as in Figure 2. In particular, the central microphone is located at $\mathbf{x}_1 = [0.5, 0.5, 0]^T$, and the remaining sensors are all located at a distance $r = 0.25$ m from \mathbf{x}_1 . If \hat{d} , $\hat{\phi}$ and $\hat{\theta}$ are the estimated plane parameters, then the localization accuracy is assessed in terms of the distance error $\varepsilon_d = d - \hat{d}$; the azimuth error $\varepsilon_\phi = \phi - \hat{\phi}$; and the co-elevation error $\varepsilon_\theta = \theta - \hat{\theta}$.

The theoretical analysis has been carried out for a set of 1500 test reflector positions, whose parameters vary on a multidimensional grid defined by: 25 values for the distance d in the range [1 m ~ 4 m]; 30 values for the azimuth ϕ in the range [0 ~ 2π]; and 2 points for the co-elevation, namely $\theta = \pi/2$ and $\theta = \pi/6$. We

assumed the error on TOA measurements to be zero-mean and Gaussian distributed with standard deviation $\sigma = 0.01 \text{ m}/c$, independent on each microphone.

Figure 3 shows the resulting theoretical standard deviation of the distance error, for all the tested reflector planes. In particular, Fig. 3-(a) is relative to the case of $\theta = \pi/2$; and Fig. 3-(b) to $\theta = \pi/6$. Similarly, Figures 4 and 5 depict the theoretical standard deviation of the azimuth error and the co-elevation error, respectively. Interestingly, for the setup under analysis, the local-

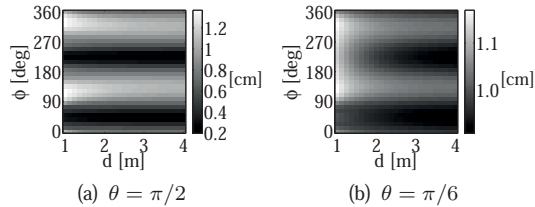


Fig. 3. Theoretical standard deviation of ε_d .

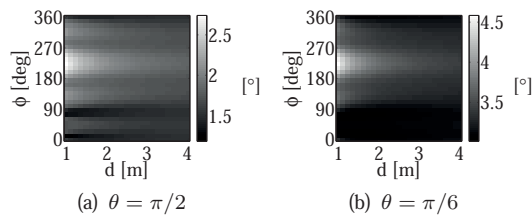


Fig. 4. Theoretical standard deviation of ε_ϕ .

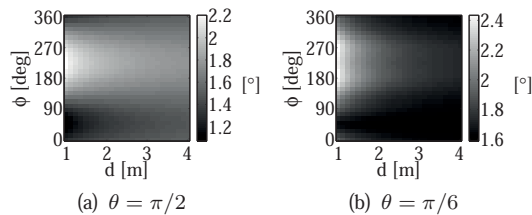


Fig. 5. Theoretical standard deviation of ε_θ .

ization accuracy is almost independent from the distance d of the reflector, while being highly variable with the azimuth ϕ . In particular, from Fig. 3 we observe that, for planes having $\phi \in [0^\circ, 90^\circ]$ or $\phi \in [180^\circ, 270^\circ]$, ε_d tends to be low while being higher for the other azimuth angles. Conversely, we notice from Fig. 4 that ε_ϕ exhibits an opposite behaviour, being higher when $\phi \in [0^\circ, 90^\circ]$ or $\phi \in [180^\circ, 270^\circ]$. Fig. 5 reveals that ε_θ has a smoother behaviour, but still presents higher values for planes with $\phi \in [180^\circ, 270^\circ]$. Finally, we observe that the accuracy tends to decrease for elevated planes, especially for the azimuth error ε_ϕ , whose average is 1.74° for $\theta = \pi/2$ and 3.34° for $\theta = \pi/6$.

5.2. Experimental evaluation

The algorithm has been tested in a small shoebox-shaped meeting room, with concrete walls and dimensions $2.77 \text{ m} \times 3.55 \text{ m} \times 3.17 \text{ m}$. The floor is covered with linoleum panels. The microphone array used in the experiment has the same geometry of that in Figure 2, and the central microphone was placed at a distance of 1.2 m from the West wall; 1.91 m from the South wall; and 1.59 m from the floor. A pc-loudspeaker was moved in 6 positions (one for each wall to be localized), emitting a MLS-sequence sampled at 48 kHz.

Consequently, $N = 7$ impulse responses are measured for each wall.

The experimental results are shown in Table 1, giving on a per wall basis, the distance error $|\varepsilon_d|$; the azimuth error $|\varepsilon_\phi|$; and the co-elevation error $|\varepsilon_\theta|$. The results are expressed with respect to the central microphone position \mathbf{x}_1 . All the reflectors are localized with high accuracy. On average, the distance error is 1.5 cm, the azimuth error 0.87° , and the co-elevation error is 0.76° . It is important to note that, for reflectors having $\theta = 0^\circ$ and $\theta = 180^\circ$ (ceiling and floor), the azimuth is not defined and therefore the co-elevation error fully characterizes the angular accuracy.

Table 1. Experimental results.

REF.	(d, ϕ, θ)	$ \varepsilon_d $ [cm]	$ \varepsilon_\phi $ [$^\circ$]	$ \varepsilon_\theta $ [$^\circ$]
West	(1.20 m, 180° , 90°)	1.3	0.49	0.62
South	(1.91 m, 270° , 90°)	0.1	1.81	1.89
East	(1.57 m, 0° , 90°)	1.1	1.09	0.22
North	(1.64 m, 90° , 90°)	4.3	0.10	0.71
Ceiling	(1.58 m, $-$, 0°)	0.9	—	0.72
Floor	(1.59 m, $-$, 180°)	1.3	—	0.38

6. CONCLUSIONS

An exact methodology for the localization of planar acoustic reflectors has been proposed. In particular, in this paper the 2D technique proposed in [5] has been extended to the case of 3D geometries. The results of the theoretical analysis reveal the applicability of the proposed method using a small number of measurements. Moreover, experimental results in a real meeting room prove that the proposed method is suitable for estimating the room geometry with high degree of accuracy.

7. REFERENCES

- [1] E. Nastasia, F. Antonacci, A. Sarti, and S. Tubaro, "Localization of planar acoustic reflectors through emission of controlled stimuli," in *European Signal Processing Conf. (EUSIPCO)*, 2011.
- [2] J. Filos, A. Canclini, F. Antonacci, A. Sarti, and P. A. Naylor, "Localization of planar acoustic reflectors from the combination of linear estimates," in *Proc. of European Signal Processing Conference (EUSIPCO)*, 2012.
- [3] S. Tervo and T. Tossavainen, "3d room geometry estimation from measured impulse responses," in *2012 IEEE International Conference on Acoustics Speech and Signal Processing (ICASSP)*, 2012.
- [4] F. Antonacci, A. Sarti, and S. Tubaro, "Geometric reconstruction of the environment from its response to multiple acoustic emissions," in *Acoustics Speech and Signal Processing (ICASSP), 2010 IEEE International Conference on*, march 2010, pp. 2822–2825.
- [5] A. Canclini, F. Antonacci, M.R.P. Thomas, J. Filos, A. Sarti, P.A. Naylor, and S. Tubaro, "Exact localization of acoustic reflectors from quadratic constraints," in *2011 IEEE Workshop on Applications of Signal Processing to Audio and Acoustics (WASPAA)*, oct. 2011, pp. 17–20.
- [6] L. Rui and K.C. Ho, "Bias analysis of source localization using the maximum likelihood estimator," in *proc. of IEEE International Conference on Acoustics, Speech and Signal Processing, ICASSP*, 2012.
- [7] B. Moran, S. D. Howard, and D. Cochran, "An information-geometric approach to sensor management," in *proc. of IEEE International Conference on Audio, Speech and Language Processing, ICASSP*, 2012.
- [8] S. Amari and H. Nagaoka, *Translations of mathematical monographs*, American Mathematical Society, 2000.
- [9] J. Filos, E. Habets, and P. Naylor, "A two-step approach to blindly infer room geometries," in *proc. of International Workshop on Acoustic Echo and Noise Cancellation, IWAENC*, 2010.
- [10] Y. A. Huang, J. Benesty, G. W. Elko, and R. M. Mersereau, "Real-time passive source localization: a practical linear-correction least-squares approach," *IEEE Transactions on Speech and audio processing*, vol. 9, no. 8, pp. 943–956, Nov. 2001.
- [11] A. Beck, P. Stoica, and Jian Li, "Exact and approximate solutions of source localization problems," *IEEE Transactions on Signal Processing*, vol. 56, no. 5, pp. 1770–1778, may 2008.
- [12] M. Compagnoni, P. Bestagini, F. Antonacci, A. Sarti, and S. Tubaro, "Localization of acoustic sources through the fitting of propagation cones using multiple independent arrays," *IEEE Transactions on Audio, Speech and Language Processing*, vol. 20, no. 7, 2012.